PRA

Lockheed

MISSILES & SPACE COMPANY

A GROUP DIVISION OF LOCKHEED AIRCRAFT C

SUNNYVALE,

38
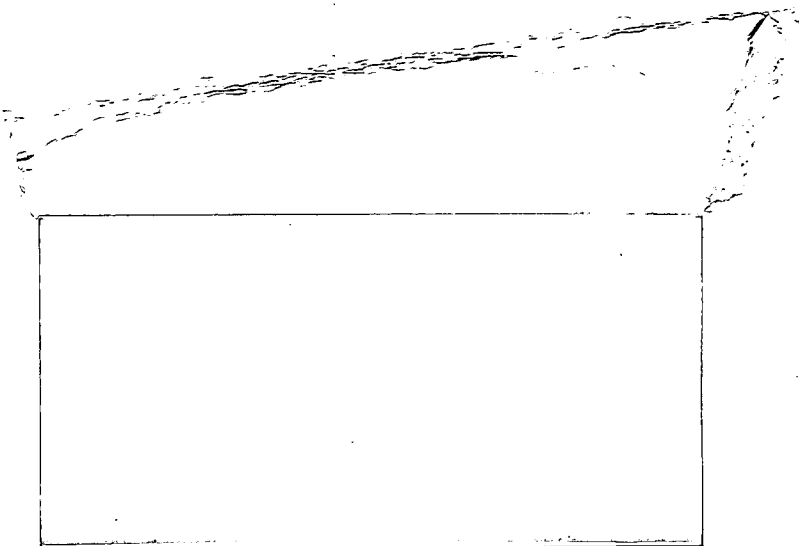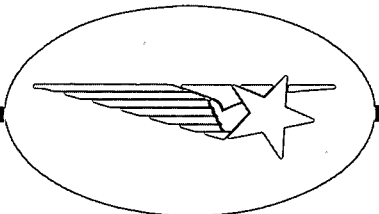
VARIATIONS OF ATMOSPHERIC DENSITY NEAR
400 KM WITH MAGNETIC ACTIVITY DURING
THE STORM PERIOD OF
28 SEPTEMBER TO 2 OCTOBER 1969

Albert D. Anderson

I

ABSTRACT

Neutral density data were obtained near 400 km (1600 LT) from a microphone density gage on OGO-6 from 0° to 40° N geomagnetic latitude for 25 September through 3 October 1969. Several geomagnetic storms occurred during this period (a_p varied from 0 to 207). Least-squares fits were made to data points on density - a_p and density - D_{st} scatter diagrams, where the density values selected were delayed in time behind a_p and D_{st}. An equation representing the least-squares fit was computed for each delay time. The equation of best fit (and the corresponding time delay between the density and the magnetic index which resulted in this best fit) was found by choosing the equation that gave the minimum standard error. For example, the best fit at 10° N geomagnetic latitude occurred for a_p at t-3 hr, where t is the time of the density values. The implications of the time differences associated with the best fits at various latitudes and longitudes are discussed with regard to the time delays involved in geomagnetic heating of the neutral upper atmosphere.

1

INTRODUCTION

The OGO-6 spacecraft was placed into an eccentric near-polar orbit (400 km perigee, 1100 km apogee, $82°$ inclination) on 5 June 1969. One of the instruments aboard is the Lockheed microphone density gage (Anderson and Sharp, 1972), designed to measure in situ variations in the neutral upper atmosphere mass density. An analysis is presented in this article based on the density data measured by this instrument at low latitudes on 110 orbits for the period 25 September through 3 October 1969. During this period the satellite perigee was between $10°$ and $25°$ N latitude at 1540 to 1630 local time. The 10.7 cm solar flux varied between 132.5 and 169.3 R.U. (Radioastronomy Units). This period was selected because several geomagnetic storms occurred. Hence, there was a large variation in the magnetic indices K_p and a_p (a_p varied from 0 to 207). This provided an opportunity to study the relationship between neutral density changes and magnetic variations at low latitudes, as a function of latitude, longitude, and time.

The U.S. Space Science Board of the National Academy of Sciences (1968) concludes that the response of the global circulation to high-latitude heating is one of the most provocative questions facing us at present. Although it is known that the density of the whole neutral upper atmosphere varies with geomagnetic activity, the relationship between the density changes and the geomagnetic activity, as represented by a_p or K_p, has not been well established. Empirical equations based on satellite-drag data are not very accurate. Transient density fluctuations

associated with geomagnetic activity are difficult to study by the satellite-drag analysis method because the time and spatial resolutions are so large. This task is also difficult because the quantity to be determined, the acceleration of the satellite's mean motion, is the second derivative of the mean anomaly. Another limitation exists because the change in the orbital period is a measure of the integrated effect of air drag in the neighborhood of perigee. Localized values of density cannot be provided, but only values averaged over an arc of 30° or more.

Another instrument on OGO-6, a quadrupole mass analyzer, was used to study neutral composition variations during the period between 27 September and 1 October 1969. These measurements by Taeusch et al (1971) provided observations of composition variability that showed a significantly different behavior of the atmosphere during a magnetic storm than the behavior deduced from the lower-resolution total mass density determined from satellite-drag measurements. The composition data indicated that the major effect of a magnetic storm on the neutral atmospheric components above 400 km altitude is localized in the high-latitude regions of the earth at magnetic latitudes above 50°, and the response time of the atmosphere to such storms is less than one hour. However, the analysis of the data from the Lockheed microphone density gage indicates that the density changes significantly with magnetic activity even at low latitudes. For example, the average density at 406 km and 1600 hr LT between 0° and 30° N latitude was 38 percent higher on 29 September 1969, a magnetically-disturbed day ($A_p = 71$) than on 27 September 1969, a quiet day ($A_p = 6$). The 10.7 cm solar flux was 151.3 R.U. on September 27 and 139.9 R.U. on September 29, where R.U. is a Radioastronomy Unit (10^{-22} w m^{-2} Hz^{-1}).

INSTRUMENT DESCRIPTION AND ACCURACY

The Lockheed microphone density gage was first flown on a satellite in January 1961 (Sharp et al, 1962). The density values measured agreed within the error of measurement with density values obtained from satellite-drag. The operating principle of this instrument lies in the transfer of momentum from the ambient neutral gas atoms and molecules, created by the relative velocity between the gas and the instrument, to the sensing element of the device, a thin metallic ribbon. This ribbon, suspended between the pole pieces of a permanent magnet to form a microphone, is mounted in the orbital-plane experimental package (OPEP) of OGO-6 looking along the velocity vector of the vehicle. The atmospheric gas, effectively having the velocity of the vehicle, exerts a pressure P on this ribbon equal to $k \rho v^2$, where k is a constant (taken to be =1) determined by the accommodation coefficient and ρ is the atmospheric density. Since the satellite velocity is independently known, the pressure is a direct measure of the density. The gas striking the ribbon is mechanically chopped by a tuning-fork chopper which interrupts the gas flow at regular intervals to produce an oscillation of the ribbon in the magnetic field of a permanent magnet, the amplitude of which is proportional to the applied pressure. The electrical voltage generated by this ribbon motion through the magnetic field is amplified and rectified to

provide a dc signal suitable for telemetry. More details concerning the instrument operation can be found in <u>Anderson and Sharp</u> (1972).

The absolute accuracy of the density values derived from the microphone gage is uncertain. A comparison made with density values derived from the mass spectrometer on OGO-6 (<u>Reber et al.</u>, 1971) using data near perigee from orbits 1640 and 1641 on 27 September 1969, showed that the density values from the microphone gage averaged 21 percent lower (<u>Anderson and Sharp</u>, 1972). <u>Reber et al</u> give no errors for their measurements, but errors in mass spectrometer measurements are estimated to be between 25 and 50 percent (<u>Nurre and DeVries</u>, 1970). Another comparison made with exospheric temperatures deduced from the profile of the 6300Å line measured from OGO-6 by <u>Blamont and Luton</u> (1970), using data from 6 perigee passes on 27 September and 28 September 1969, showed that temperatures derived from the microphone density gage data averaged 6.3 percent lower. Blamont and Luton state an accuracy of $\pm 50^{\circ}$K for their temperature.

It appears that the microphone density gage measures relative density variations accurately. The average difference in density at 406 km at a given geomagnetic latitude from 0° to 30°N between 28 successive orbits on 25, 26 and 27 September 1969 ($K_p \leq 3$) was 9.0 percent. A total of 60 pairs of density values were used to

calculate the differences; the two density values in a given pair

differed in time by about 100 minutes and in longitude by about

25 degrees.

DENSITY VERSUS K_p (OR a_p)

Figure 1 shows some typical latitudinal density profiles for

27-30 September 1969 at 406 km and 1600 Hr local time from about 0°

to 40^ON for K_p equal to 0,4+, 6 and 8, respectively. These density

profiles are fitted to density points derived from the microphone

density measurements (Anderson and Sharp, 1972), made over an alti-

tude range near perigee averaging about 20 km. An atmospheric

model (Anderson and Francis, 1966) was used to normalize the data to

an altitude of 406 km. The resulting data points in Figure 1 have an

average time separation of one-half minute and an average distance sep-

aration of 2 to 3 degrees. The 10.7 cm solar flux varied slightly

during 27-30 September 1969, from 151.3 R.U. to 137.0 R.U. The curves

of Figure 1 indicate that the 406 km density definitely increased at all

latitudes with increasing geomagnetic activity, represented by K_p. The aver-

age density from 10° N to 20° N is over twice as great for $K_p = 8$ as $K_p = 0$.

The curve for $K_p = 8$ (orbit 1684) indicates a broad maximum with three

peaks from 15° N to 35° N. Many curves from other orbits during

25 September - 3 October 1969 present a similar broad maximum, with much lower densities near the equator and above 40° N, especially those curves associated with high K_p, indicating geomagnetic disturbed conditions. This low-latitude density bulge, which seems to be a permanent feature near the equinoxes, was first found by analyzing drag data from Explorer 1 in 1961 and 1962 (Anderson, 1966). Newton and Pelz (1969), analyzing in-situ density measurements from Explorer 32 density gages for May through October 1966 during geomagnetically quiet days, concluded that the low midlatitude density can be 20 percent greater than the equatorial density during the day for altitudes between 300 and 400 km. Hedin and Mayr (1971) found maxima in the N_2 and O densities measured by the mass spectrometer on OGO-6 at $\pm 20^{\circ}$ magnetic latitude during July and September 1969.

The low-latitude density bulge illustrated in Figure 1 may prove important for understanding the semi-annual effect appearing in satellite drag data. This effect is poorly understood at present. It is well known that there is a greater frequency of geomagnetic disturbances around the equinoxes. On the average, "magnetic" heating is indicated to be stronger near the Fall equinox than near the Spring equinox, with a minimum of heating from June to August and December to January. These features are also characteristic of the semi-annual effect. Based on this similarity, a recent explanation advanced for the semi-annual effect proposes that it is a complex effect resulting from both latitudinal density variations caused by solar heating and "magnetic" heating, with the former dominating during summer and winter and the latter dominating during Spring and Fall (Anderson, 1969).

Figure 2 shows two curves for the period 27-30 September 1969, where the solid curve is the density at 406 cm and 20° N geomagnetic latitude and the dashed curve is for K_p. From inspection, it is obvious that the higher densities are usually associated with high K_p. The coefficient of correlation between density and K_p is $r = +.97$. K_p is interchangeable with a_p, as indicated on the right hand side of Figure 2.

METHOD

Inasmuch as Figure 2 indicated a good correlation between density and K_p (or a_p), a method was devised to derive predictive equations. The method consists in making least-squares straight-line fits to points on density a_p scatter diagrams, where the density ρ at 400 km is delayed in 3-hr time intervals behind a_p from 0 to 24 hr. Equations of the fitted straight lines were derived for all the delay times for a given latitude or longitude sector. The corresponding standard error was calculated for each equation. The delay time which resulted in the best fit at a given latitude or longitude sector was found by selecting the equation having the minimum standard error. Hence, the best-fit equation was taken as that which resulted in minimum standard error.

The equation of the least-squares straight line fit for the ρ, a_p points is

$$\rho_c = (a + b\ a_p)\ 10^{-15}\ \text{gm cm}^{-3}. \tag{1}$$

The constants a and b are determined from the following normal equations:

$$\sum \rho = n\ a + b \sum a_p \tag{2}$$

$$\sum (\rho \ a_p) = a \sum a_p + b \sum a_p^2 , \qquad (3)$$

where n is the number of data points.

Solving (2) and (3),

$$a = \frac{\sum (\rho \ a_p)}{\sum a_p} + \frac{\sum a_p \sum \rho \sum a_p^2 - n \sum (\rho \ a_p) \sum a_p^2}{n \sum a_p \sum a_p^2 - (\sum a_p)^3} ; \qquad (4)$$

and,

$$b = \frac{n \sum (\rho \ a_p) - \sum a_p \sum \rho}{n \sum a_p^2 - (\sum a_p)^2} . \qquad (5)$$

The standard deviation of the n data points about the line (1), or the standard error is,

$$S_\rho = \left[\frac{(\rho - \rho_c)^2}{n} \right]^{1/2} . \qquad (6)$$

Equations (1), (4), (5) and (6) were programmed for computer calculation. For example, Figure 3 is a scatter diagram containing 80 data points at $10°N$ geomagnetic latitude from 26 September through 3 October 1969. The ordinate is ρ at 400 km in units of 10^{-15} gm cm^{-3}, and the abscissa is a_p' or the value of a_p at t - 3 hr, t being the time of the density values. The a_p' values range from 0 to 207 ($K_p = 8$), while ρ ranges from about 4.0 to 14.5 x 10^{-15} gm cm^{-3}. The equation of the least-squares solid line in Figure 3 is

$$\rho_c = (5.46 + .0336 \ a_p') \ 10^{-15} \ \text{gm cm}^{-3} . \qquad (7)$$

The dashed straight lines in Figure 3 indicate the limits of the standard error, which is

$$S_\rho = 1.07 \times 10^{-15} \text{ gm cm}^{-3},\tag{8}$$

or 16.0 percent of the average density. Some of the points contained outside the dashed straight lines are associated with peaks and troughs appearing in the latitudinal density profile (Figure 1).

The index a_p comes entirely from converting K_p to a normalized linear scale. The 3-hr planetary index K_p is obtained by averaging values from 12 observatories located between 47.7 and 62.5 geomagnetic latitude, averaging 56 degrees geomagnetic latitude. Thus a_p (or K_p) represent magnetic disturbances near 56 degrees geomagnetic latitude. The fact that a_p and K_p represent a mixture of disturbance effects associated with auroral electrojets, storm-time variations, and other magnetic variations of smaller amplitude such as sudden impulses makes them useful for very general correlations. However, for more discriminating studies it is desirable to have indices for each type of disturbance. Since we are interested in low-latitude effects, it was decided to investigate the Equatorial D_{st} magnetic activity index (Hess, 1965; Siguira and Cain, 1969). Equatorial D_{st} is a measure of the mean departure from normal of the horizontal component, H, of the Earth's magnetic field observed at a group of low-latitude stations, whereas a_p is based on 3-hr ranges of the field at stations in higher latitudes.

Accordingly, the D_{st} magnetic index was selected to find if more accurate least-squares fits could be achieved on density versus D_{st} scatter diagrams. Not only does the type of magnetic storm variation represented by D_{st} occur at low and moderate latitudes, but the D_{st} values themselves are available every hour, instead of every 3 hours like a_p. This could be an advantage when studying the relationship of magnetic storms with rapid changes in the density. However, D_{st} can be positive or negative. The negative values, especially the larger ones, are normally associated with ring-current particle injection associated with magnetic storms.

The equation for the least-squares straight line fit for the ρ, D_{st} points is

$$\rho_c = (a' + b'D_{st}) \ 10^{-15} \ gm \ cm^{-3} \qquad , \qquad (9)$$

where the constants a' and b' are determined from normal equations similar to (4) and (5) with D_{st} substituted for a_p.

As an example, Figure 4 is a scatter diagram of density at 400 km versus D_{st} at t hr, corresponding to 89 density data points at 20°N (Figure 3). The D_{st} values range from -113 to 45. The equation of the least-squares straight line is

$$\rho_c = (6.51 - .0256 \ D_{st}) \ 10^{-15} \ gm \ cm^{-3}. \qquad (10)$$

The standard error is

$$S_\rho = 1.69 \times 10^{-15} \ gm \ cm^{-3} \qquad , \qquad (11)$$

or 23.6 percent of the average density.

$\mathcal{C}$

DATA ANALYSIS

Table 1 presents the constants a and b in Equation 1 computed from

(4) and (5) for a_p from time t to t - 24 hr in 3-hr increments and geo-

magnetic latitudes $0°$ N, $10°$ N, $20°$ N, $30°$ N, and $40°$ N and all latitudes ($0°$ N to

$40°$ N). Table 2 exhibits the corresponding standard error S_ρ, expressed in

percent of the average density of the n data points, calculated from (6)

and (1). In addition, S_ρ is given for a_p < 15 and a_p > 15, representing

quiet and disturbed geomagnetic conditions, respectively. The minimum

standard error in each column is marked with an asterisk. This value can

be used to determine the time delay between ρ and a_p that gives the

best correlation in a given column. For example, under the $10°$ N

column the minimum S_ρ occurs for a_p at t - 3 hr. The corresponding a and

b selected from Table 1 results in Equation 7 (see Figure 3). Displayed at

the bottom of each column in Table 2 is the average S_ρ, the ratio of the

average S_ρ to the minimum S_ρ, the number of data points n, and the relative

density (density for "all latitudes" = 1.00). The minimum S_ρ occurs at

$0°$ N, $10°$ N, and $20°$ N for a_p at t - 3 hr and at $30°$ N and $40°$ N for a_p at t-9

hr. However, no significance is attached to the minimum values at $30°$ N and

$40°$ N because the average/minimum S_ρ ratios are low. It doesn't matter greatly

Table 1

a AND b FOR LATITUDE AND TIME

TIME OF a_p (hr)	GEOMAGNETIC LATITUDE										
	0° N		10° N		20° N		30° N		40° N		ALL LATITUDES
	a	b	a	b	a	b	a	b	a	b	a	b
t	5.12	.0297	5.72	.0261	6.06	.0289	6.18	.0278	6.87	.0151	5.95	.0271
t-3	5.24	.0262	5.46	.0336	5.80	.0371	6.26	.0241	6.65	.0184	5.78	.0303
t-6	5.45	.0226	5.68	.0289	5.84	.0369	6.16	.0271	6.72	.0145	5.87	.0287
t-9	5.66	.0207	6.02	.0215	6.00	.0339	6.17	.0294	6.59	.0184	6.03	.0271
t-12	5.58	.0231	6.04	.0196	6.05	.0300	6.31	.0232	7.08	.0081	6.11	.0231
t-15	5.45	.0360	6.12	.0179	6.29	.0245	6.52	.0187	7.03	.0090	6.23	.0207
t-18	5.44	.0287	5.88	.0265	6.34	.0231	6.52	.0194	6.89	.0137	6.16	.0230
t-21	5.60	.0193	5.93	.0262	6.63	.0149	6.83	.0110	7.19	.0087	6.38	.0167
t-24	5.72	.0173	6.10	.0195	6.63	.0152	6.93	.0086	7.16	.0107	6.44	.0154

Table 2

a_p, STANDARD ERROR FOR LATITUDE AND TIME

TIME OF a_p (hr)	GEOMAGNETIC LATITUDE					ALL LATITUDES	ALL LATITUDES ($a_p < 15$)	ALL LATITUDES ($a_p > 15$)
	0° N	10° N	20° N	30° N	40° N			
t	15.7	21.5	21.2	18.9	13.9	20.3	21.2	18.9
t-3	14.1*	16.0*	15.5*	19.4	13.9	17.5*	16.8	16.8*
t-6	19.3	20.3	16.7	18.4	14.4	19.1	16.5*	19.3
t-9	22.2	24.5	19.8	18.0*	13.2	21.0	19.0	20.4
t-12	21.6	24.6	20.6	20.0	15.3	21.8	21.0	20.8
t-15	20.0	24.8	22.4	21.2	14.8	22.4	21.8	20.8
t-18	20.6	23.7	23.4	21.5	13.5	22.4	21.2	21.6
t-21	22.4	23.7	25.2	23.1	15.5	24.0	22.0	22.6
t-24	23.4	24.8	25.2	23.6	15.7	24.3	22.8	22.7
AVE.	19.9	22.6	21.1	20.4	14.4	21.4	20.2	20.4
AVE/MIN	1.41	1.41	1.36	1.13	1.09	1.22	1.23	1.22
n	49	80	89	80	30	328	171	157
REL. DENSITY	.89	.96	1.03	1.04	1.08	1.00	.89	1.12

*Minimum.

which time delay is selected for a_p for these latitudes. As indicated at the bottom of Table 2, the relative density is slightly below normal for the lower latitudes and for "all latitudes" with $a_p < 15$, while it is slightly above normal for the higher latitudes and for "all latitudes" with $a_p > 15$.

Table 3 gives the constants a and b for 60-degree longitude sectors and for all longitudes (same as the "all latitude" column in Table 1). Table 4 presents the corresponding S_ρ. The average/ minimum S_ρ ratio for $180°E - 240°E$ is 1.81. The minimum S_ρ occurs for a_p at t-3 hr. Hence, it is very advantageous to use a_p at t-3 hr and a and b in Table 3 at t-3 hr in Equation 1 for this sector. On the other hand, it doesn't matter very much which time delay is used for a_p in the $60°E - 120°E$ sector since the average/ minimum S_ρ ratio is only 1.11. As indicated at the bottom of Table 4, the relative density variation with longitude is slight between $0°N$ and $40°N$ geomagnetic latitude.

Table 5 gives the constants a' and b' (Equation 9) computed for D_{st} for times t to t-12 hr in 1-hr increments and geomagnetic latitudes $0°N$, $10°N$, $20°N$, $30°N$, $40°N$ and "all latitudes" ($0°N-40°N$). Table 6 presents the corresponding standard error S_ρ. The minimum standard error (marked with an asterisk) occurs for D_{st} at time t, the same times as the density values, for each latitude except $10°N$, where it occurs with a time delay of 2 hours. Yet, the average/minimum S_ρ ratios at the bottom of Table 6 are low, so not much confidence can be placed in any particular time delay.

Table 3

a AND b FOR LONGITUDE AND TIME

TIME OF a_p (hr)	LONGITUDE													ALL LONGITUDES	
	$0°-60°E$		$60°-120°E$		$120°-180°E$		$180°-240°E$		$240°-300°E$		$300°-360°E$				
	a	b	a	b	a	b	a	b	a	b	a	b		a	b
t	5.53	.0375	5.99	.0140	5.59	.0340	5.72	.0296	6.17	.0202	5.95	.0459		5.92	.0271
t-3	5.30	.0342	6.24	.0137	5.93	.0220	5.41	.0357	5.60	.0484	5.76	.0400		5.78	.0303
t-6	5.60	.0310	6.57	.0035	5.73	.0356	5.27	.0577	5.69	.0409	5.60	.0339		5.87	.0287
t-9	6.23	.0199	6.59	.0041	5.50	.0503	5.08	.0753	5.54	.0310	5.95	.0329		6.03	.0271
t-12	6.30	.0175	5.93	.0288	5.54	.0448	5.42	.0379	5.74	.0209	6.45	.0291		6.11	.0231
t-15	6.21	.0218	6.41	.0117	5.67	.0295	5.84	.0237	5.85	.0332	6.88	.0139		6.23	.0207
t-18	6.04	.0317	6.49	.0071	5.65	.0197	5.39	.0542	6.28	.0202	6.68	.0197		6.16	.0230
t-21	5.96	.0384	6.08	.0138	5.96	.0147	6.08	.0331	6.58	.0090	6.56	.0297		6.38	.0167
t-24	5.81	.0319	6.03	.0131	6.36	.0091	6.82	.0048	6.13	.0240	6.55	.0366		6.44	.0154

Table 4

a_p, STANDARD ERROR FOR LONGITUDE AND TIME

TIME OF a_p (hr)	LONGITUDE						ALL LONGITUDES
	0°-60° E	60°-120° E	120°-180° E	180°-240° E	240°-300° E	300°-360° E	
t	19.6	14.5	13.0*	21.7	20.4	20.7	20.3
t-3	15.8*	15.7	14.0	13.5*	17.6*	19.3	17.5*
t-6	17.2	17.0	13.1	14.5	18.8	16.2*	19.1
t-9	22.0	17.2	14.5	20.3	17.6*	18.8	21.0
t-12	22.3	14.6	15.4	26.6	18.5	22.7	21.8
t-15	20.9	16.7	17.0	28.9	19.2	24.5	22.4
t-18	21.9	17.0	17.0	22.4	21.4	22.9	22.4
t-21	22.3	14.9	19.1	29.6	22.7	23.2	24.0
t-24	20.9	14.2*	21.2	33.2	20.0	24.0	24.3
AVE.	20.3	15.8	16.0	24.5	19.6	21.4	21.4
AVE./MIN	1.28	1.11	1.23	1.81	1.11	1.32	1.22
n	65	50	55	49	45	64	328
REL. DENSITY	1.02	0.97	0.96	1.00	1.00	1.06	1.00

*Minimum.

Table 5

a' AND b' FOR LATITUDE AND TIME

TIME OF D_{st} (hr)	GEOMAGNETIC LATITUDE											ALL LATITUDES	
	0° N		10° N		20° N		30° N		40° N				
	a'	b'	a'	b'	a'	b'	a'	b'	a'	b'	a'	b'	
											a'	b'	
t	5.96	-.0245	6.28	-.0238	6.51	-.0256	6.65	-.0177	6.82	-.0170	6.37	-.0239
t-1	5.99	-.0218	6.29	-.0244	6.55	-.0249	6.78	-.0145	6.98	-.0139	6.42	-.0227
t-2	5.97	-.0202	6.30	-.0239	6.64	-.0213	6.95	-.0095	7.20	-.0096	6.50	-.0198
t-3	5.99	-.0177	6.36	-.0204	6.74	-.0175	7.07	-.0062	7.22	-.0101	6.58	-.0166
t-4	5.99	-.0163	6.37	-.0192	6.79	-.0153	7.15	-.0037	7.29	-.0079	6.62	-.0148
t-5	5.99	-.0140	6.40	-.0167	6.87	-.0120	7.27	.0001	7.48	-.0011	6.69	-.0114
t-6	6.00	-.0136	6.43	-.0150	6.90	-.0107	7.30	.0011	7.50	-.0004	6.73	-.0102
t-7	6.02	-.0107	6.46	-.0126	6.92	-.0095	7.27	.0003	7.42	-.0033	6.74	-.0093
t-8	6.01	-.0105	6.45	-.0131	6.95	-.0085	7.31	.0014	7.37	-.0053	6.75	-.0088
t-9	6.03	-.0094	6.47	-.0121	6.97	-.0081	7.30	.0013	7.41	-.0038	6.77	-.0080
t-10	6.04	-.0086	6.48	-.0114	6.97	-.0080	7.27	.0001	7.43	-.0030	6.77	-.0078
t-11	6.01	-.0105	6.47	-.0126	6.96	-.0083	7.25	-.0005	7.40	-.0037	6.76	-.0086
t-12	6.02	-.0114	6.46	-.0131	6.95	-.0090	7.20	-.0020	7.40	-.0034	6.74	-.0094

Table 6

D_{St}, STANDARD ERROR FOR LATITUDE AND TIME

TIME OF D_{St} (hr)	GEOMAGNETIC LATITUDE					ALL LATITUDES
	0° N	10° N	20° N	30° N	40° N	
t	21.2*	24.3	23.6*	22.6*	14.8*	22.7*
t-1	21.9	24.2	23.8	23.0	15.5	23.2
t-2	22.1	24.0*	24.6	23.5	15.7	23.6
t-3	23.0	25.1	25.2	23.8	15.6	24.3
t-4	23.7	25.5	25.7	24.0	15.9	24.7
t-5	24.3	26.0	26.1	24.0	16.3	25.3
t-6	24.5	26.3	26.2	24.0	16.3	25.4
t-7	25.0	26.6	26.4	24.0	16.1	25.4
t-8	25.0	26.4	26.5	24.0	16.1	25.6
t-9	25.1	26.6	26.5	24.0	16.1	25.6
t-10	25.1	26.6	26.5	24.0	16.1	25.6
t-11	25.0	26.4	26.5	24.0	16.1	25.4
t-12	25.0	26.4	26.4	24.0	16.1	25.4
AVE.	23.9	25.7	25.7	23.8	15.9	24.8
AVE./MIN	1.13	1.07	1.09	1.05	1.07	1.09
n	49	80	89	80	30	328
REL. DENSITY	.89	.96	1.03	1.04	1.08	1.00

*Minimum.

Table 7 shows the constants a' and b' for 60-degree longitude sectors and "all longitudes." The constant b' is positive in the 60°E to 120°E from t hr to t-5 hr and in the 180°E to 240°E sector from t-8 hr to t-10 hr. This indicates that there is no correlation between density and D_{st} during these delay times at these longitudes. Table 8 presents the S_ρ corresponding to Table 7. The correlation between density and D_{st} is good only at certain longitudes and delay times, as indicated by large values of the average/ minimum S_ρ ratios at the bottom of the table—in the 120°E to 180°E and 180°E to 240°E sectors with time delays of 4 hr and 0 hr, respectively. The standard error is low at 16.5 percent for D_{st} from t to t-12 hr in the 60°E to 120°E sector. For some reason, there is little or no correlation between density and D_{st} in this sector. The same is true for density and a_p (Table 4). Since changes in D_{st} do not result in appreciable changes in density, the scatter of points in the scatter diagram is less, resulting in low standard error. The relative density values at the bottom of Table 8 indicates that there is not much variation of density with longitude, as pointed out before.

DISCUSSION

Table 9 gives a comparison between the standard error resulting using a_p (Table 2) and D_{st} (Table 6) for geomagnetic latitude and delay times of 0, 3, 6, 9, and 12 hr. In all cases, the standard error is lower using a_p than D_{st}, averaging 19.3 percent lower. Also, the average/minimum S_ρ ratios

Table 7

a' AND b' FOR LONGITUDE AND TIME

TIME OF D_{st}(hr)	0°-60°E a'	0°-60°E b'	60°-120°E a'	60°-120°E b'	120°-180°E a'	120°-180°E b'	180°-240°E a'	180°-240°E b'	240°-300°E a'	240°-300°E b'	300°-360°E a'	300°-360°E b'	ALL LONGITUDES a'	ALL LONGITUDES b'
t	6.60	-.0246	6.74	.0009	6.17	-.0222	5.66	-.0383	5.46	-.0388	6.94	-.0179	6.37	-.0239
t-1	6.64	-.0250	6.78	.0028	6.10	-.0228	5.61	-.0414	5.75	-.0317	6.98	-.0186	6.42	-.0227
t-2	6.77	-.0187	6.76	.0015	5.99	-.0223	5.67	-.0391	6.39	-.0164	7.05	-.0187	6.50	-.0198
t-3	6.74	-.0178	6.76	.0018	5.88	-.0238	5.50	-.0448	6.62	-.0110	7.22	-.0111	6.58	-.0166
t-4	6.63	-.0217	6.74	.0007	5.82	-.0237	5.96	-.0358	6.64	-.0114	7.21	-.0132	6.62	-.0148
t-5	6.61	-.0199	6.74	.0006	5.82	-.0254	6.54	-.0168	6.52	-.0171	7.26	-.0092	6.69	-.0114
t-6	6.70	-.0169	6.70	-.0009	5.96	-.0217	6.49	-.0186	6.47	-.0210	7.29	-.0064	6.73	-.0102
t-7	6.60	-.0176	6.69	-.0011	6.06	-.0173	6.83	-.0058	6.62	-.0173	7.23	-.0102	6.74	-.0093
t-8	6.60	-.0158	6.67	-.0017	5.93	-.0194	7.01	.0032	6.77	-.0111	7.23	-.0098	6.75	-.0088
t-9	6.51	-.0166	6.69	-.0013	6.30	-.0098	7.03	.0055	6.74	-.0151	7.28	-.0055	6.77	-.0080
t-10	6.45	-.0162	6.71	-.0006	6.60	-.0012	7.02	.0074	6.76	-.0124	7.23	-.0080	6.77	-.0078
t-11	6.38	-.0185	6.70	-.0009	6.63	-.0001	6.83	-.0112	6.85	-.0063	7.23	-.0077	6.76	-.0086
t-12	6.39	-.0171	6.76	.0010	6.58	-.0022	6.87	-.0122	6.79	-.0094	7.18	-.0092	6.74	-.0094

LONGITUDE

Table 8

D_{St}, STANDARD ERROR FOR LONGITUDE AND TIME

TIME OF D_{St} (hr)	LONGITUDE						ALL LONGITUDES
	0°-60° E	60°-120° E	120°-180° E	180°-240° E	240°-300° E	300°-360° E	
t	24.6	16.5	18.2	18.7*	19.8*	25.3*	22.7*
t-1	24.5	16.5	17.2	19.2	21.1	25.5	23.2
t-2	25.6	16.5	15.8	21.1	23.2	25.5	23.6
t-3	25.5	16.5	15.2	24.0	23.4	26.0	24.3
t-4	24.9	16.5	15.1*	29.9	23.4	25.9	24.7
t-5	24.9	16.5	17.0	32.8	22.7	26.1	25.3
t-6	25.5	16.5	19.3	32.5	22.6	26.3	25.4
t-7	24.9	16.5	20.3	33.3	23.2	26.1	25.4
t-8	24.9	16.5	20.0	33.3	23.4	26.1	25.6
t-9	24.5	16.5	21.4	33.3	23.2	26.3	25.6
t-10	24.1	16.5	21.8	33.3	23.4	26.1	25.6
t-11	23.6*	16.5	21.8	33.2	23.9	26.1	25.4
t-12	24.1	16.5	21.5	33.0	23.6	26.0	25.4
AVE.	24.7	16.5	18.8	29.0	22.8	25.9	24.8
AVE./MIN	1.08	1.00	1.44	1.78	1.21	1.04	1.09
n	65	50	55	49	45	64	328
REL. DENSITY	1.02	.97	.96	1.00	.99	1.06	1.00

*Minimum.

Table 9

a_p AND D_{St}, STANDARD ERROR FOR LATITUDE AND TIME

TIME OF a_p AND D_{St} (hr)	GEOMAGNETIC LATITUDE										ALL LATITUDES	
	0°N		10°N		20°N		30°N		40°N			
	a_p	D_{St}	a_p	D_{St}	a_p	D_{St}	a_p	D_{St}	a_p	D_{St}	a_p	D_{St}
t	15.7	21.1*	21.5	24.3*	21.1	23.6*	18.9	22.6*	13.9	14.8*	20.3	22.7*
t-3	14.1*	23.0	16.0*	25.1	15.5*	25.2	19.4	23.8	13.9	15.6	17.5*	24.3
t-6	19.3	24.5	20.3	26.3	16.7	26.2	18.4	24.0	14.4	16.3	19.1	25.4
t-9	22.2	25.1	24.5	26.6	19.8	26.5	18.0*	24.0	13.2*	16.1	21.0	25.6
t-12	21.6	25.0	24.6	26.4	20.6	26.4	20.0	24.0	15.3	16.1	21.8	25.4
AVE.	18.6	23.7	21.4	25.7	18.7	25.6	18.9	23.7	14.1	15.8	19.9	24.7
AVE./MIN	1.32	1.12	1.34	1.06	1.21	1.08	1.05	1.05	1.07	1.07	1.14	1.09
n	49	49	80	80	89	89	80	80	30	30	328	328

*Minimum.

are appreciably higher for a_p than D_{st} at $0°$ N, $10°$ N, and $20°$ N. For these

latitudes, the minimum standard error for a_p occurs at t-3 hr, where it

averages 37.8 percent lower than that for D_{st} at the same time delay. There-

fore, it appears that the density can be predicted best at low latitudes

using a_p at t-3 hr, at least during the period under consideration.

Table 10 shows a comparison between standard errors resulting from

using a_p (Table 4) and D_{st} (Table 8) for 60-degree longitude sectors and

all longitudes ($0°$ - $360°$E) for delay times 0, 3, 6, 9, and 12 hr. In all

longitude sectors the average standard error is lower using a_p than D_{st},

averaging 21.2 percent lower. Based on the average/minimum S_ρ ratio only,

a_p is clearly superior to D_{st} for predictive purposes in the $0°$ to $60°$E

and $300°$ to $360°$E sector with time delays of 3 and 6 hr, respectively. D_{st}

appears better at $120°$ - $180°$E at t-3 hr. The high value of both average/

minimum S_ρ ratios in the $180°$ to $240°$E sector indicates that the density is

well correlated in this sector with both a_p and D_{st}, with time delays of

3 and 0 hr, respectively. The low values of both ratios in the $60°$ to $120°$E

and $240°$ to $300°$E sectors indicates that density is poorly correlated with

both a_p and D_{st}. In these sectors it seems preferable to use a_p since it

results in a lower standard error.

In Table 2 the minimum standard error occurs for a_p at t-3 hr at $0°$ N, $10°$ N, and

$20°$ N. No significance is attached to the fact that the minimum S_ρ occurs at t-9 hr

at $30°$ AND $40°$ N

because the average/minimum S_ρ ratios are low for these latitudes. The density at

Table 10

a_p AND D_{St}, STANDARD ERROR FOR LONGITUDE AND TIME

TIME OF a_p AND D_{St} (hr)	LONGITUDE												ALL LONGITUDES	
	0°-60°E		60°-120°E		120°-180°E		180°-240°E		240°-300°E		300°-360°E			
	a_p	D_{St}	a_p	D_{St}	a_p	D_{St}	a_p	D_{St}	a_p	D_{St}	a_p	D_{St}	a_p	D_{St}
t	19.6	24.6	14.5*	16.5	13.0*	18.2	21.7	18.7*	20.4	19.8*	20.7	25.3*	20.3	22.7*
t-3	15.8*	25.5	15.7	16.5	14.0	15.2*	13.5*	24.0	17.6*	23.4	19.3	26.0	17.5*	24.3
t-6	17.2	25.5	17.0	16.5	13.1	19.3	14.5	32.5	18.8	22.6	16.2*	26.3	19.1	25.4
t-9	22.0	24.5	17.2	16.5	14.5	21.4	20.3	33.3	17.6	23.2	18.8	26.3	21.0	25.6
t-12	22.3	24.1*	14.6	16.5	15.4	21.8	26.6	33.0	18.5	23.6	22.7	26.0	21.8	25.4
AVE.	19.4	24.8	15.8	16.5	14.0	19.2	19.3	28.3	18.6	22.5	19.5	26.0	19.9	24.7
AVE./MIN	1.23	1.03	1.09	1.00	1.08	1.26	1.43	1.51	1.06	1.14	1.21	1.03	1.14	1.09
n	65	65	50	50	55	55	49	49	45	45	64	64	328	328

*Minimum.

$0° - 20°N$ may correlate best with the a_p value 3 hr earlier because there

is a time delay of about 3 hr between the peak geomagnetic activity in the

auroral zone and the atmospheric response at low latitudes. If the main

atmospheric heating is caused by some mechanism or energy source in the

auroral regions, then wave propagation could transport the energy from the

auroral region to the equatorial region within a time interval of about

3 hr. Jacchia and Slowey (1967) from satellite-drag analysis, give a mean

time delay of 7.2 ± 0.3 hr for an average latitude of 25 degrees. However,

the inaccuracies associated with satellite-drag measurements have been dis-

cussed already (Also, see Taeusch et al.,1971).

De Vries (1971), reporting on neutral density data obtained from the

Low-G Calibration System (LOGACS) flown on a polar orbiting satellite during

a period of high geomagnetic activity (May 22-26, 1967), states that the

in-situ high resolution data show that the density increases almost simul-

taneously with enhanced geomagnetic activity. The largest density increases

occurred in the region of the maximum current of the auroral electrojet with

no significant increases in the equatorial region until several hours later.

Atmospheric waves, apparently associated with joule heating, appear to orig-

inate in the auroral region at altitudes lower than 150 km and propagate up-

ward and toward the Equator. Blamont and Luton (1970) analyzed thermospheric

temperature measurements from data obtained by a Fabry-Perot interferometer

on OGO-6 in the period 26 September-6 October 1969, during which two large

geomagnetic disturbances occurred. These temperature measurements showed a

$300°K$ increase in the two polar regions while the temperature near the Equator

increased by only $90°K$.

Volland and Mayr (1971) calculated the response of thermospheric density during geomagnetic disturbance, assuming that an impulse type of heat input is injected into a small band of latitude within the auroral oval during local nighttime. They calculated the temporal response of the thermospheric density to the heat input. This theory indicates a dependence of the atmospheric density changes on latitude and longitude. The general trend of the density variations is in agreement with the trend observed in the LOGACS observations (DeVries, 1971). The data in Table 4 indicate that there is a good correlation between density and a_p at t-3 hr at $180°$ to $240°$E and little or no correlation at $60°$ to $120°$E and $240°$ to $300°$E. Table 8 indicates good correlation between density and D_{st} between $180°$ to $240°$E with no time delay and little or no correlation between $60°$ to $120°$E.

May and Miller (1971) have shown from a rather limited sample of satellite spin-rate data that the variations in density at 310 km in low latitudes are more closely indicated by Equatorial D_{st}, with a 2-hr lag of density behind D_{st}, than by a_p with the 7-hr lag suggested by Jacchia and Slowey (1967). The improvement of the relationship with D_{st} as compared with a_p is most marked in the recovery phase following the peaks of magnetic storms. At these times the density recovers more slowly than a_p, in common with D_{st}. May and Miller state that it is not possible with their data to test whether or not the improvement was caused by the density being measured in low latitudes, where the magnetic observations from which Equatorial D_{st} is evaluated are made. The minimum S_p values in Table 6 indicate no lag in time between

density and D_{st}, except at 10° N, where it is 2 hr. According to <u>De Vries</u> (1971), the density increases simultaneously with a_p in auroral latitudes, near where a_p is measured. If this is true, it appears reasonable to expect that likewise no lag should occur between the density and D_{st} at low latitudes, where D_{st} is measured, provided that the geomagnetic disturbance causes worldwide heating simultaneously. The 3-hr lag between the density at low latitudes and a_p (Table 2) could result from the fact that most of the energy is initially deposited in auroral latitudes and later transported southwards by wave or bulk mass motion.

CONCLUSIONS

This analysis shows that marked density increases occur at low latitudes during geomagnetic storms. The average density from 10° N to 20° N is over twice as great for $K_p = 8$ as $K_p = 0$. The best least-squares fit and corresponding delay time between density and a magnetic index can be determined for a given latitude or longitude sector from the minimum standard error. The average/ minimum standard error ratio indicates whether or not there is a good correlation between the density and the magnetic index having the time delay associated with the minimum standard error. Large average/minimum standard error ratios occur at 0° N, 10° N, and 20° N geomagnetic latitude where the minimum standard error occurs for a_p at t-3 hr. The average/minimum ratio is very large in the longitude sector 180° to 240° E, where the minimum standard error occurs at a time delay of 3 hr between density and a_p.

With regard to density and D_{st}, the best correlation at low latitudes results with no time delay, except at $10°N$, where it is 2 hr. Like a_p, the the best correlation with longitude occurs at $180°$ to $240°E$. In most cases, the correlation of density with D_{st} is not as good as that with a_p, as indicated by the magnitudes of the standard errors and average/minimum ratios. It appears that the density can be predicted best at low latitudes using a_p at t-3 hr. If the minimum values of the standard error reflect the time delay between the onset of a storm (as indicated by a_p and D_{st}), then inasmuch as there is little or no lag between density and D_{st} and about a 3 hr lag between density and a_p, this indicates that a geomagnetic disturbance causes worldwide heating simultaneously, with most of the heating ensuing in the auroral zones, some of which is later transported to low latitudes.

These results are valid for $0°N$ to $40°N$ geomagnetic latitude for the period 25 September through 3 October 1969 for an altitude of 400 km, 1600 local time, and solar flux of 145 R.U. Equations 7 and 10 can be used for other altitudes, local times, and solar activity by normalizing them with the aid of a model atmosphere (See Anderson and Francis, 1966). If the explanation given in Anderson (1969) for the semi-annual effect is correct, then this effect is automatically taken into account. The general applicability of the predictive equations can only be determined by analyzing density data from other periods having geomagnetic storms.

ACKNOWLEDGMENT

REFERENCES

Anderson, A.D.; Existence of a significant latitudinal variation in
density from 200 to 800 kilometers, Nature, 209, 656, 1966.

Anderson, A.D.; A model for the semi-annual effect appearing in the
drag data of satellites in eccentric orbits, Lockheed Missiles and
Space Co. Report, LMSC 6-78-69-37 (N70-23721), 1969.

Anderson, A.D. and W.E. Francis; The variation of the neutral atmos-
pheric properties with local time and solar activity from 100 to
10,000 km, J. Atmospheric Sci., 23, 110, 1966.

Anderson, A.D. and G.W. Sharp; Neutral density measurements near 400
kilometers by a microphone density gage on OGO-6 during 12-15 July
1969, J. Geophys. Res., 77, 1878, 1972.

Blamont, J.E. and J.M. Luton; OGO-VI direct measurements and monitor-
ing of the temperature of the neutral atmosphere from 200 to 350
km of altitude: the magnetic storm of Sept-Oct 1969, Centre National
de la Recherche Scientifique Rept. f. 18, 1970.

DeVries, L.L.; Structure and motion of the thermosphere shown by den-
sity data from the low-G accelerometer calibration system (LOGACS),
URSI/COSPAR Meeting, June 24-26, 1971, Seattle, Washington, 1971.

Hedin, A.E. and H.G. Mayr; Magnetic control of neutral thermospheric
density near the equator, Trans. Amer. Geophys. Union, 52, 872, 1971.

Hess, W.N.; Introduction to Space Science, Gordon and Breach Science
Publishers, New York, 1965.

Jacchia, L.G. and J. Slowey; Geomagnetic perturbations and upper-
atmosphere heating, J. Geophys. Res., 72, 1423, 1967.

May, B.R. and D.E. Miller; The correlation between air density and
magnetic disturbance deduced from changes of satellite spin-rate,
Planet. Space Sci., 19, 39, 1971.

Newton, G.P. and D.T. Pelz; Latitudinal variations in the neutral atmos-
pheric density, J. Geophys. Res., 74, 4169, 1969.

Nurre, G.S. and L.L. DeVries; An experiment to determine density
variations in the earth's atmosphere and other atmospheric and
aerodynamic information, Fourth National Conference on Aerospace
Meteorology, May 4-7, 1970, Las Vegas, Nevada, 1970.

Reber, C.A., D. N. Harpold, R. Horowitz and A.E. Hedin; Horizontal
distribution of helium in the earth's upper atmosphere, J. Geophys.
Res., 76, 1845, 1971.

Sharp, G.W., W.B. Hanson and D.D McKibbin; Atmospheric density measure-
ments with a satellite-borne microphone gage, J. Geophys. Res., 67,
1375, 1962.

Siguira, M. and S.J. Cain; Provisional hourly values of Equatorial
Dst for 1964, 1965, 1966 and 1967, NASA Goddard Space Flight Center
Rept. X-612-69-20 (N69-20074), 1969.

Taeusch, D.R., G.R. Carignan, and C.A. Reber; Response of the neutral
atmosphere to geomagnetic disturbances, Space Res., 9, 995, 1971.

U.S. Space Science Board, Physics of the Earth in space, National Research
Council, National Academy of Sciences, 1968.

Volland, H. and H.G. Mayr; Response of the thermospheric density to
auroral heating during geomagnetic disturbances, J. Geophys. Res.,
76, 3764, 1971.

FIGURE CAPTIONS

FIGURE 1   Some typical latitudinal density profiles for 27-30 September 1969 at 406 km and 1600 LT from $0°$ to $40°$ N latitude for K_p = 0, 4+, 6, and 8. These density profiles are fitted to density points derived from the Lockheed microphone density gage measurements (<u>Anderson and Sharp</u>, 1972).

FIGURE 2   Density and K_p versus Universal Time (U.T.) for 27 September through 30 September 1969. The solid curve is the density at 406 km and $20°$N geomagnetic latitude, and the dashed curve is for K_p. The correlation coefficient between density and K_p is r = +.97. The values of K_p (and the corresponding a_p) are shown on the right.

FIGURE 3   Density at 400 km versus a_p' scatter diagram for 80 data points for 26 September - 3 October 1969 at $10°$N geomagnetic latitude, 1600 LT, and 145 R.U., where a_p' is the value of a_p at t-3 hr, t being the time of the density values. The solid straight line represents the least-squares fit to the data points (Equation 7). The standard error (Equation 8) limits are indicated by the dashed straight lines.

FIGURE 4   Density at 400 km versus D_{st} scatter diagram for 89 data points for 26 September — 3 October 1969 at $20°$N geomagnetic latitude, 1600 LT, and 145 R.U., where D_{st} is at time t, t being the time of the density values. Equation 10 is the equation of the solid least-square fit line. Equation 11 represents the standar error whose limits are indicated by the dashed lines.
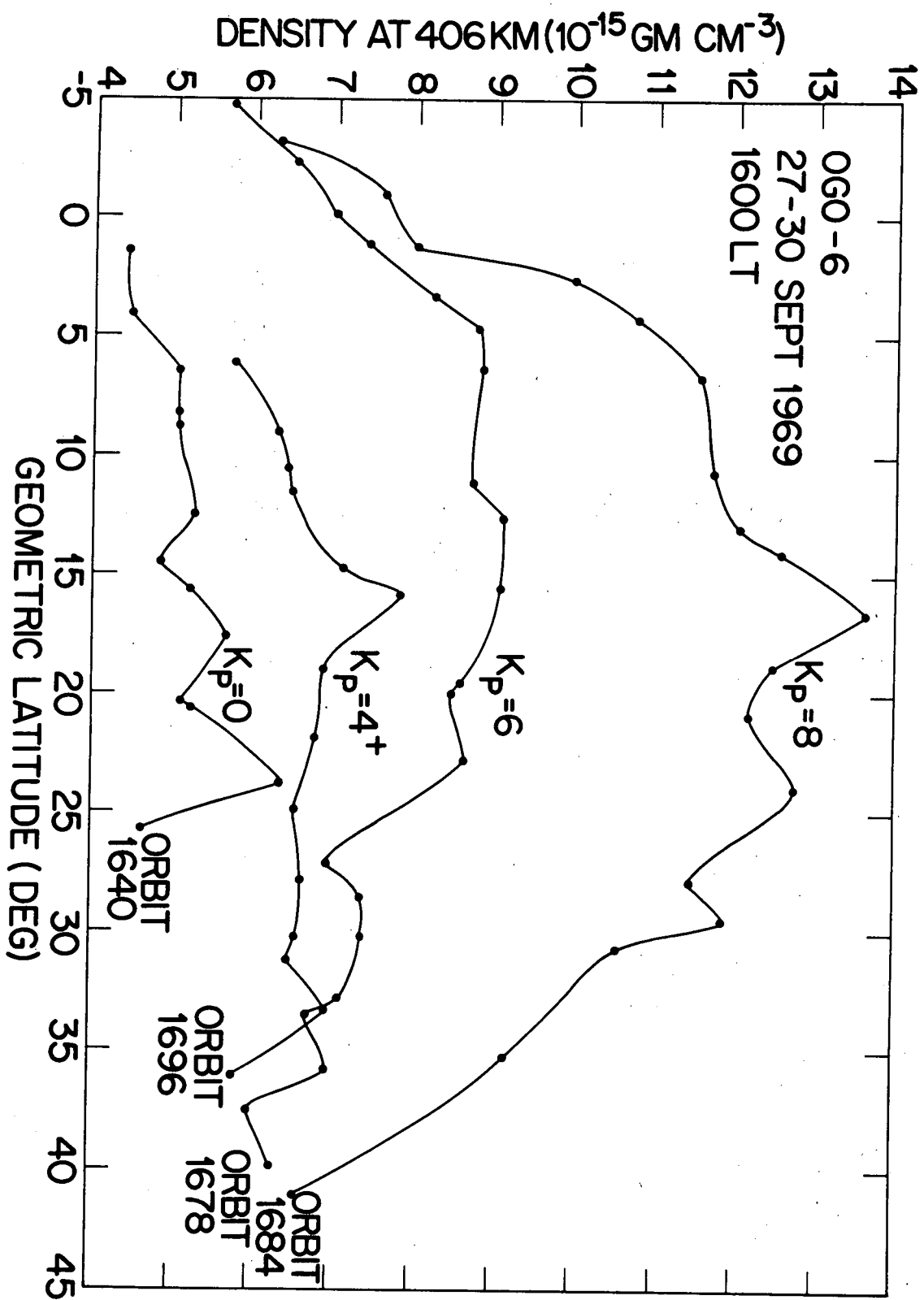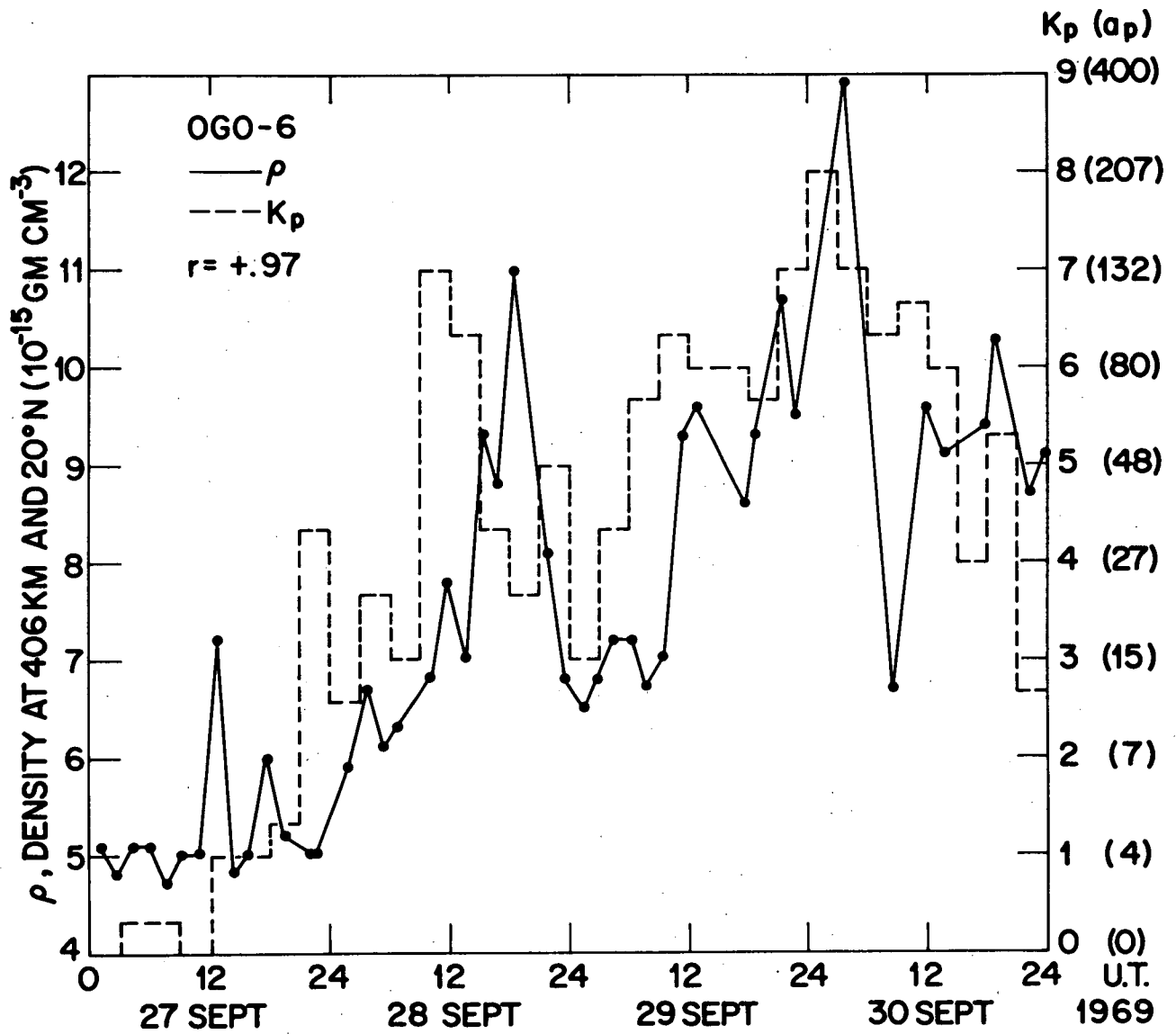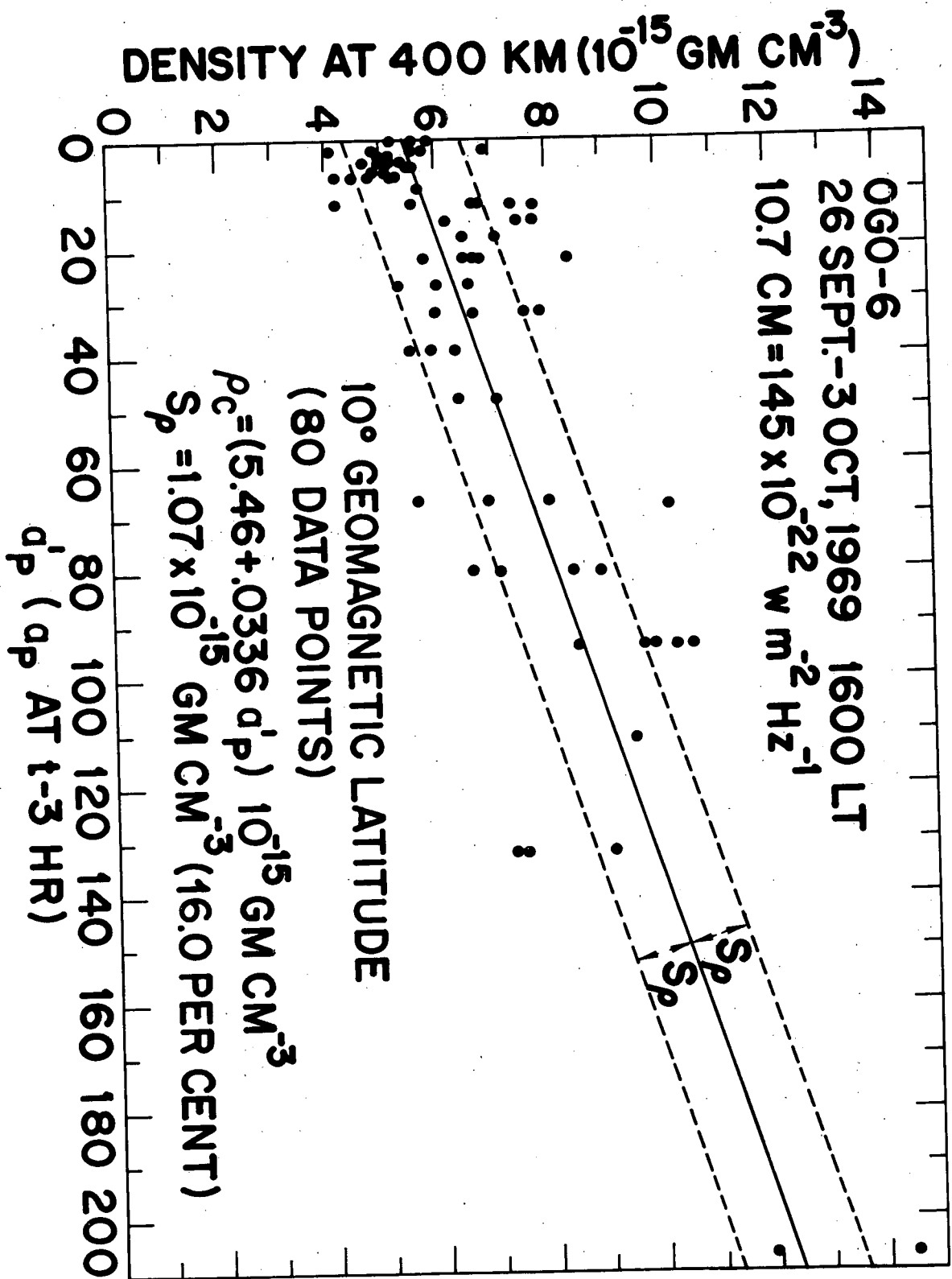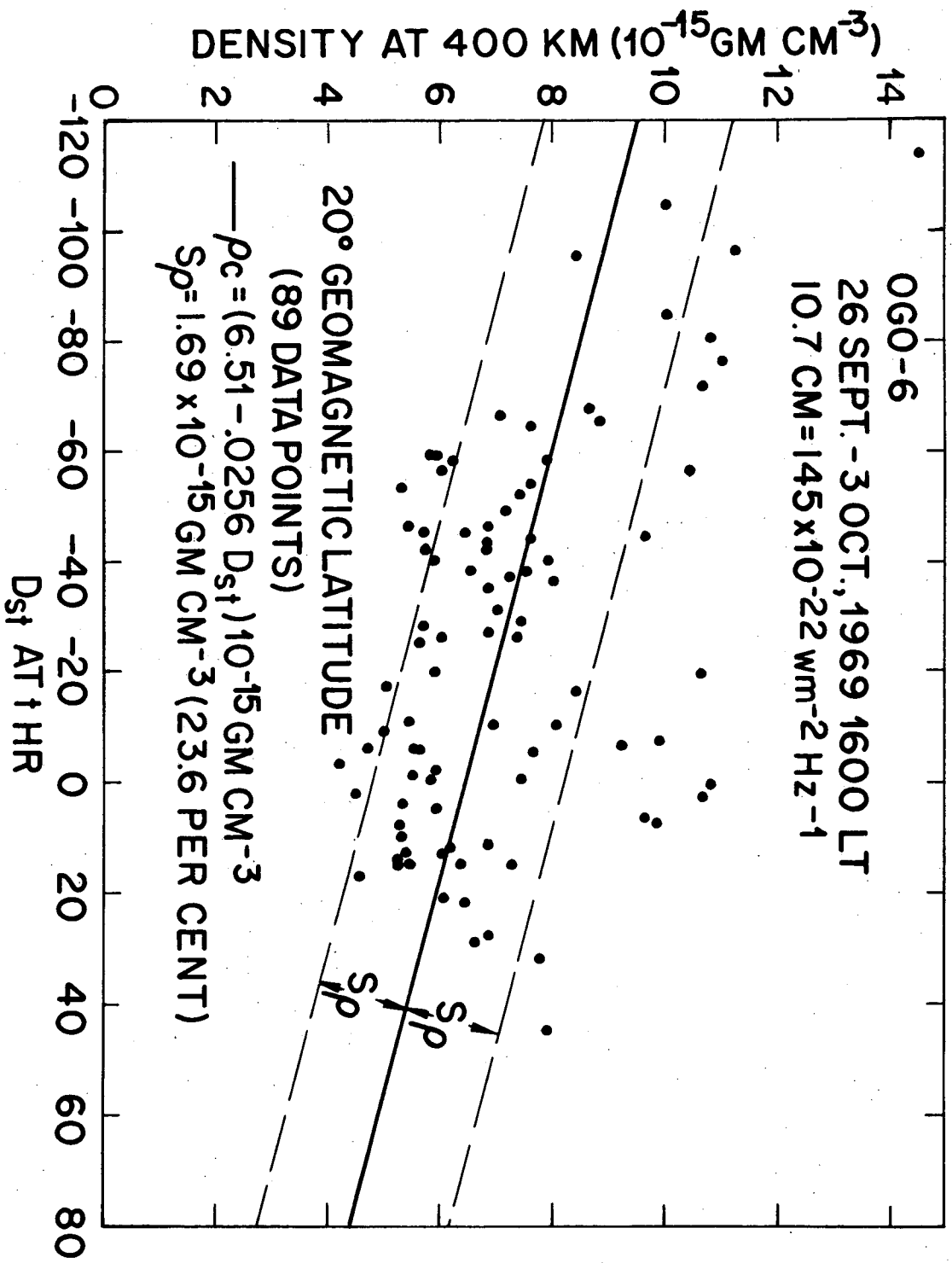
DENSITY AT 406 KM (10^{-15} GM CM^{-3})

OGO-6
27-30 SEPT 1969
1600 LT

$K_P = 0$

$K_P = 4^+$

$K_P = 6$

$K_P = 8$

ORBIT 1640

ORBIT 1696

ORBIT 1678

ORBIT 1684

GEOMETRIC LATITUDE (DEG)

Fig. 1

Fig. 2

OGO-6
26 SEPT.-3 OCT., 1969 1600 LT
10.7 CM=145×10^{-22} w m^{-2} Hz^{-1}

10° GEOMAGNETIC LATITUDE
(80 DATA POINTS)
ρ_c=(5.46+.0336 a'_p) 10^{15} GM CM^{-3}
S_ρ =1.07×10^{-15} GM CM^{-3} (16.0 PER CENT)

DENSITY AT 400 KM (10^{-15}GM CM^{-3})

a'_p (a_p AT t-3 HR)

S_ρ

S_ρ

Fig. 3

Fig. 4